



The role of tin species in doped iron (III) oxide for photocatalytic degradation of methyl orange dye under UV light

Nurul Affiqah Arzaee^a, Nadia Betti^b, Ahmed Al-Amiery^a,
Wan Nor Roslam Wan Isahak^{a,*}

^a Department of Chemical and Process Engineering, Faculty of Engineering and Built Environment, Universiti Kebangsaan Malaysia, 43600 UKM Bangi, Selangor, Malaysia

^b Materials Engineering Department, University of Technology-Iraq, P.O. Box: 10001, Baghdad, Iraq

ARTICLE INFO

Keywords:

Photocatalysis
Sol-gel
Sn-doped nanocomposites
Optical properties
Dye degradation

ABSTRACT

Iron (III) oxide, a stable semiconductor with versatile applications, was synthesized alongside Sn-doped Fe₂O₃ (Sn-Fe₂O₃) using the sol-gel technique. Characterization via X-ray diffraction, field-emission scanning electron microscopy, and UV-visible spectroscopy confirmed the presence of α - and γ -Fe₂O₃ phases in the synthesized powders. Incorporation of the dopant reduced the initial band gap energy of Fe₂O₃ (2.2 eV) by approximately 0.1 eV. To evaluate photocatalytic performance, Fe₂O₃ and Sn-Fe₂O₃ were tested for decolorization efficiency of a methyl orange solution. Results revealed the 5 wt% Sn-doped catalyst as optimal, achieving complete degradation of methyl orange within 120 min under simulated solar light. The addition of small amounts of Sn effectively reduced the Fe₂O₃ band gap and significantly enhanced photocatalytic performance. Investigation of pH and dye concentration impact on photocatalytic degradation revealed superior activity under acidic conditions compared to alkaline. Furthermore, maintaining a moderate concentration of methyl orange (10 ppm) ensured optimum photocatalytic activity.

1. Introduction

Wastewater treatment using photocatalysis with semiconductor materials has several advantages over conventional treatment methods. Photocatalysis is known for its low energy consumption, absence of secondary compound production, and lower operational costs compared to other chemical processes [1,2]. Fe₂O₃, an n-type semiconductor, has been of interest to scientists for its application as a photocatalyst in the photodegradation of wastewater containing dyes. This is due to its small band gap value of 2.2 eV, which allows for the absorption of both ultraviolet and visible light, indirectly enhancing its photocatalytic efficiency. While the percentage of ultraviolet light in the solar spectrum only covers 5%, visible light accounts for up to 43% of the total electromagnetic rays from the sun [3]. One of the challenges in the actual photocatalyst environment is the isolation, collection, and recovery of photocatalysts from the wastewater stream. To address this issue, researchers have turned to heterogeneous photocatalysts, such as Fe₂O₃, which possess natural magnetic properties that allow for easy recovery with the presence of an external magnet [4]. Additionally, Fe₂O₃ can be synthesized at a relatively low cost, as iron is the fourth most abundant element on earth, and it is non-toxic, making it a suitable material for wastewater treatment [5]. However, Fe₂O₃ exhibits less efficient photocatalytic activity due to its short hole diffusion property, which is approximately 2 nm–4 nm. This weakness can be overcome through the dopant technique [6]. To improve the

* Corresponding author.

E-mail address: wannorroslam@ukm.edu.my (W.N. Roslam Wan Isahak).

<https://doi.org/10.1016/j.heliyon.2023.e18076>

Received 5 May 2023; Received in revised form 29 June 2023; Accepted 5 July 2023

Available online 7 July 2023

2405-8440/© 2023 Published by Elsevier Ltd.

This is an open access article under the CC BY-NC-ND license

(<http://creativecommons.org/licenses/by-nc-nd/4.0/>).

photodegradation of Fe₂O₃, it has been doped with several potential elements, such as Ti, Al, Zn, Mo, and Cr [7]. Previous studies have shown that carbonaceous compounds can significantly enhance the dye decolorization process at ambient conditions [8], and using nanoengineering approaches to design materials can improve photocatalytic performance [9]. In addition, Sn- α -Fe₂O₃ has been reported to have excellent activity in the photocatalytic water-splitting reaction [10]. However, further studies are needed to determine the loading effect of Sn on α -Fe₂O₃ to improve its performance and life cycle.

This study aims to investigate the role of Sn as a dopant on Fe₂O₃ for the photodegradation of methyl orange. The physical and chemical properties of the photocatalysts will be analyzed using various techniques. The photodegradation performance of the Sn-based photocatalysts will also be investigated using several reaction parameters, such as pH value, dye concentration, and type of photocatalysts. The significant effect of Sn doping content will be elaborated and compared with the non-doping photocatalyst.

2. Experimental

Fe(NO₃)₃·9H₂O (nonahydrate) and SnCl₂ (anhydrate) were obtained from R&M Chemicals and Ajax Chemical, respectively. C₆H₈O₇·H₂O and C₂H₅OH (99.5%) were supplied by System Company. Polyethylene glycol (PEG) 300 was obtained from Merck. For the photocatalytic activity study, methyl orange (C₁₄H₁₄N₃NaO₃S) was obtained from Riedemann Schmidt. Fe₂O₃ and Sn-Fe₂O₃ photocatalysts with different dopant percentages, such as 0.5%, 3%, 5%, and 8%, were synthesized using the sol-gel method.

To synthesize Fe₂O₃ material, 3 g of iron (III) nitrate was dissolved in 50 ml of deionized water and 50 ml of ethanol. The solution was then stirred at room temperature on a hot plate with a magnetic stirrer. After 30 min, 1 ml of PEG was added to the solution and continuously stirred. Approximately 3 g of citric acid was then dissolved in the mixture of 25 ml of deionized water and 25 ml of ethanol and dropped into the previous mixture and stirred for 2 h. The mixture was heated in an oven overnight at 100 °C. The product formed was ground into powder before calcining at 400 °C for 2 h. The same procedure was used to synthesize Sn-Fe₂O₃ with different loading percentages of 0.5%, 3%, 5%, and 8%. SnCl₂ was initially dissolved in the mixture of ethanol and deionized water and PEG. The synthesized photocatalysts were labeled as Fe₂O₃, 0.5% Sn-Fe₂O₃, 3% Sn-Fe₂O₃, 5% Sn-Fe₂O₃, and 8% Sn-Fe₂O₃.

The crystal structures of Fe₂O₃ and Sn-Fe₂O₃ were characterized using X-ray diffractogram (XRD) (K α Cu rays, 1.5406Å) in 2 θ scanning ranging from 10° to 80°. The morphological properties of the samples were also examined using field emission-scanning electron microscopy (FE-SEM). The band gap and optical properties of Fe₂O₃ and Sn-Fe₂O₃ were measured using a UV spectrophotometer PerkinElmer and Lambda 69 software.

To study the photodegradation of the dye solution using photocatalytic reaction in the presence of Sn-Fe₂O₃, we used 60 ml of methyl orange solution at the concentration of 10 ppm. The solution without the catalyst was placed under UV light as a control, followed by others in the presence of catalysts.

Initially, the dye solutions and catalysts were stirred for 20 min at room temperature in a closed and dark environment. The photocatalytic reaction was performed under a simulated sunlight system (Xenon lamp) with a light intensity of 1000 W/m². Approximately 2 ml of aliquot was obtained every 30 min and centrifuged at 14500 rpm. The dye solution was then analyzed using a UV spectrometer to measure the decolorization. Methyl orange decolorization for each sample was determined using Equation (1) below. The photocatalytic reaction of dyes was then studied using 0.5% Sn-Fe₂O₃, 3% Sn-Fe₂O₃, 5% Sn-Fe₂O₃, and 8% Sn-Fe₂O₃. Parameters, such as dye concentrations and pH value (reaction condition), were studied in detail.

$$\text{Decolorization (\%)} = \frac{(A_0 - A_t)}{A_0} \times 100\% \quad (1)$$

where A₀ and A_t are the initial and final absorptions of dyes, respectively.

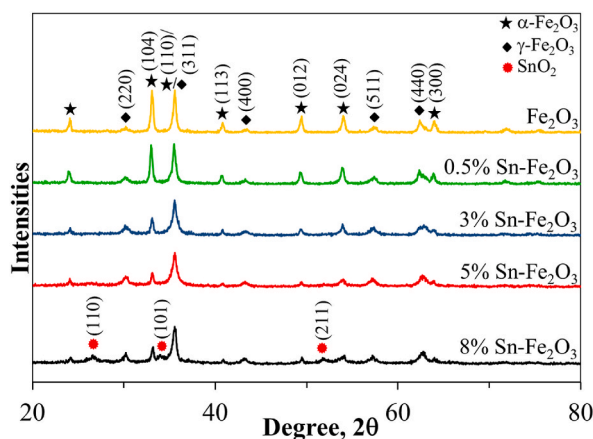


Fig. 1. XRD pattern for Fe₂O₃ and Fe₂O₃-doped Sn catalysts that was synthesized using sol-gel method.

3. Results and discussion

3.1. Effect of Sn loading

To identify the crystal properties of the photocatalysts, XRD analysis was performed. This technique allowed us to analyze the effect of Sn dopant on the crystal structure. The XRD pattern for the photocatalysts, including Fe_2O_3 , 0.5% Sn- Fe_2O_3 , 3% Sn- Fe_2O_3 , 5% Sn- Fe_2O_3 , and 8% Sn- Fe_2O_3 , is shown in Fig. 1.

Fig. 1 shows the XRD pattern with Bragg's degree between 20° and 80° of the crystal that was synthesized using sol-gel method. From the peaks of XRD pattern for pristine Fe_2O_3 , the pattern was perfectly matched with the combination of two different phases of Fe_2O_3 . The first phase is recognized as $\alpha\text{-Fe}_2\text{O}_3$ (JCPDS No. 33-0664), whereas their peaks were recorded at the 2θ value of 24.08° , 33.08° , 35.58° , 40.80° , 49.45° , 54.00° , and 63.90° , which were the basis for the angle of Miller index of (012), (104), (110), (113), (024), (116), and (300), respectively. The peaks at 2θ value of 30.20° , 35.58° , 43.48° , 57.33° , and 62.38° were based at the angle of Miller index of (220), (311), (400), (511), and (440), which represented to the phase of $\lambda\text{-Fe}_2\text{O}_3$ (JCPDS No. 39-1346), respectively. The growth of these two phases of Fe_2O_3 may be due to the calcination temperature of these materials during synthesis at 400°C [11]. Fig. 1 shows that the XRD peaks intensity for $\alpha\text{-Fe}_2\text{O}_3$ were clearly decreasing by the Sn loading amount on Fe_2O_3 crystals. The presence of Sn element inhibited the $\alpha\text{-Fe}_2\text{O}_3$ crystallization. The morphology of the 5% Sn- Fe_2O_3 nanoparticles was studied using FE-SEM. Fig. 2 (a)–(d) show the images of 5% Sn- Fe_2O_3 in different magnification scales. The 5% Sn- Fe_2O_3 photocatalyst consisted of spherical-structured nanoparticles where all the particles were conjoined together to form porous pores. The nanoparticle size means were tabulated between 30 nm and 40 nm.

The optical characterization results, such as band gap value of photocatalyst, can be generated from UV-Visible Spectroscopy. Light absorption can measure the band gap of the catalysts. Light absorption spectrum for the photocatalysts, namely Fe_2O_3 , 0.5% Sn- Fe_2O_3 , 3% Sn- Fe_2O_3 , 5% Sn- Fe_2O_3 , and 8% Sn- Fe_2O_3 , are depicted in Fig. 3(a). The bandgap of each photocatalyst was determined from Tauc Plot, as shown in Fig. 3(b), and its value was measured by the straight-line correlation intercept with x axis on Tauc plot. Band gap for pristine Fe_2O_3 was obtained at 2.20 eV, which was in the range of the value reported by several researchers [7,12]. This value represented light absorption with wavelength of 564 nm and less. The bandgap value was dramatically decreased to 2.06, 2.08, and 2.09 eV for the Fe_2O_3 catalyst with 0.5%, 3%, and 5% of Sn doping, respectively. However, the band gap value was then increased to 2.20 eV at the Sn dopant loading up to 8%. This decreasing pattern of the bandgap enabled it to absorb more light and subsequently create more electron-hole pair and enhanced the direct degradation process of dye via the OH^\bullet degradation mechanism.

Pristine Fe_2O_3 and Fe_2O_3 -doped Sn that were synthesized in this work were tested in methyl orange degradation reaction under simulated sunlight, and the stage of degradation was monitored using UV-Vis spectrometer. The calculation of decolorization percentage using equation (1). Photodegradation percentage for 10 ppm methyl orange solution and the pH value of 5.3 without photocatalyst loading or with photocatalyst are summarized in Table 1. It showed that 5% Sn- Fe_2O_3 catalyst was successfully achieved highest photodegradation percentage at 100%. While, at higher loading of Sn species of 8% showed a relatively lower photodegradation performance.

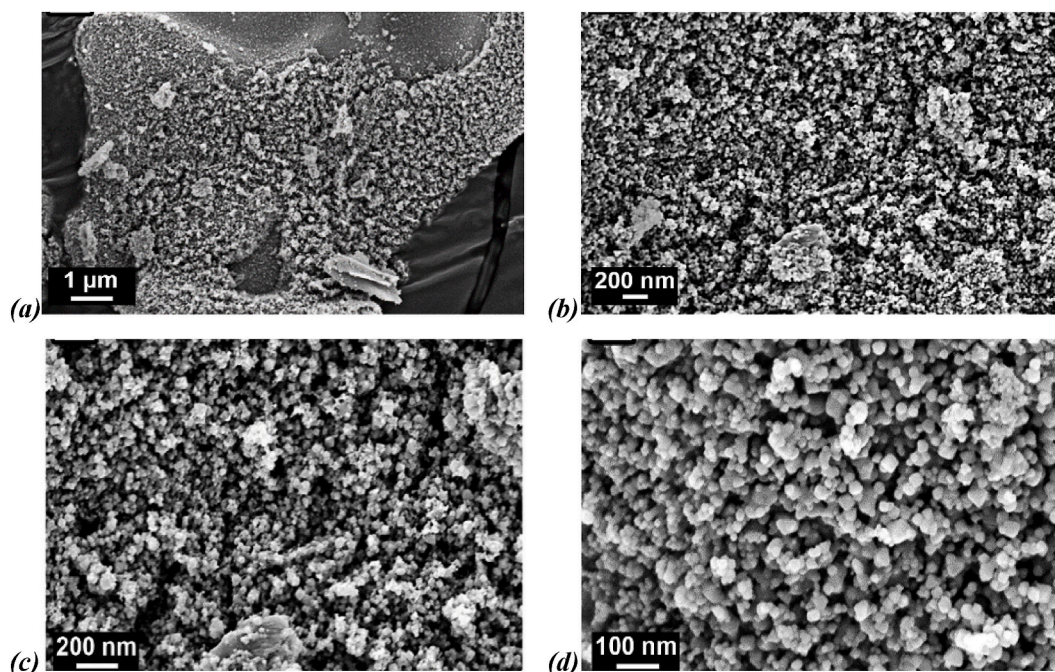


Fig. 2. FE-SEM micrographs for 5% Sn- Fe_2O_3 photocatalyst. Magnification scale of (a) 1:10000, (b) 1:30000, (c) 1:50000, and (d) 1:100000.

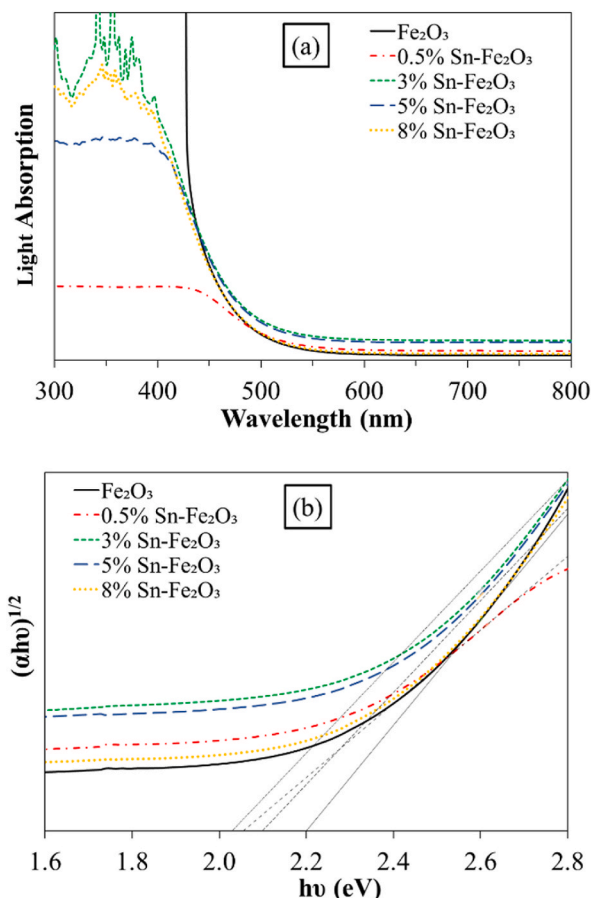


Fig. 3. (a) Light absorption spectra for (a) pristine Fe₂O₃, Fe₂O₃-doped Sn, and, (b) Tauc plot to determine the band gap of pristine Fe₂O₃ and Fe₂O₃-doped photocatalysts.

Results of light absorption of the solution without or with catalyst for 120 min are illustrated in Fig. 4 (a). In this figure, high absorption rate represented the high concentration of methyl orange, which is less degradable. By contrast, the low intensity UV-Vis signal represented the high degradation rate of methyl orange to form a colorless solution. The presence of the Fe₂O₃-based catalysts showed a faster degradation rate than the control sample without catalyst. The decolorization performance was dramatically increased by the loading of Sn dopant ranging from 0.5% to 5%. As a result, methyl orange solution was then fully degraded in the presence of 5% Sn-Fe₂O₃ after 2 h under UV light irradiation. The degradation rate showed a relative decrease in its performance when 8% Sn was loaded on Fe₂O₃. The high content of Sn at 8% loading changed the surface properties of the catalyst by covering the Fe₂O₃ surface and subsequently reduced the active site on the surface. The performance of the degradation reaction without and with the 5% Sn-Fe₂O₃ catalysts at different UV irradiation times ranging from 0 min to 120 min is depicted in Fig. 4 (b). The irradiation time is shown to play a significant role in the degradation reaction, and it is observed that all the dyes were fully degraded after 120 min. This finding highlights the effectiveness of the catalyst in promoting the degradation of methyl orange under UV light irradiation. The gradual decrease in absorption over time indicates the progressive degradation of the dye molecules, leading to a decrease in their concentration. The use of the 5% Sn-Fe₂O₃ catalyst facilitates the photodegradation process, resulting in a faster and more efficient degradation of methyl orange compared to the reaction without the catalyst.

Table 1

Methyl orange decolorization without or with the presence of several type of Fe₂O₃ photocatalysts.

Photo- catalyst Time (min)	Without catalyst (Control)	Fe ₂ O ₃	0.5% Sn-Fe ₂ O ₃	3% Sn-Fe ₂ O ₃	5% Sn-Fe ₂ O ₃	8% Sn-Fe ₂ O ₃
	Decolorization percentage (%)					
0	0	0	0	0	0	0
30	0	22	31	35	43	26
60	1	51	59	66	75	46
90	4	69	76	84	93	72
120	11	79	90	93	100	88

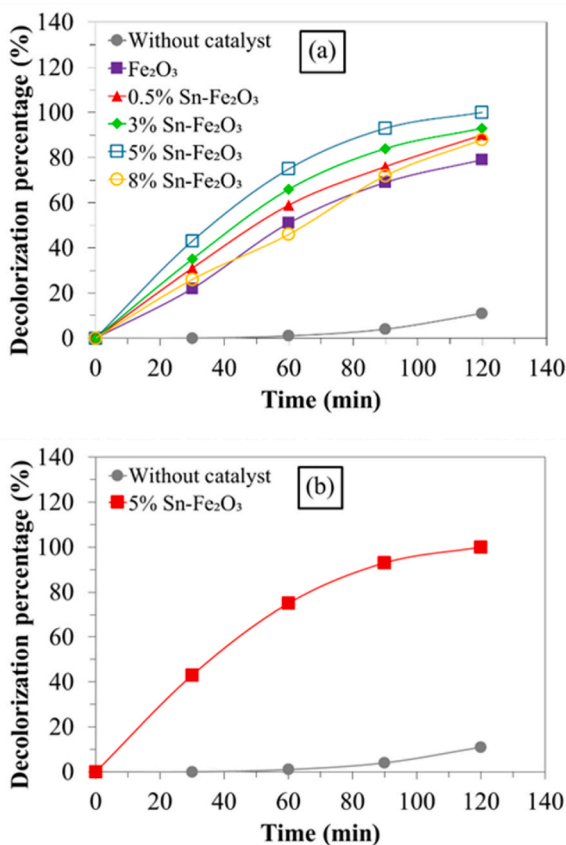


Fig. 4. (a) Photodegradation performance of dye solutions without or with the presence of photocatalyst after 120 min and (b) photodegradation performance without and in the presence of 5% $\text{Sn-Fe}_2\text{O}_3$ for 120 min.

3.2. Effect of pH value

In other situations, the environment and system of dye solution can significantly influence the degradation over photocatalysts. Early screening studies showed that 5% $\text{Sn-Fe}_2\text{O}_3$ gives a tremendous performance in methyl orange degradation. This photocatalyst was then further studied in effect of the different of pH value and dye concentration towards decolorization rate. Methyl orange degradation reaction with dye concentration of 10 ppm was studied in acidic and basic conditions of pH 5.3 and 9.6, respectively. Fig. 5 shows the percentages of methyl orange decolorization at different pH values. According to Fig. 5, the acidic condition enhanced the dye degradation more effectively than basic condition in the presence of Fe_2O_3 -doped Sn catalysts. At acidic condition, the dye

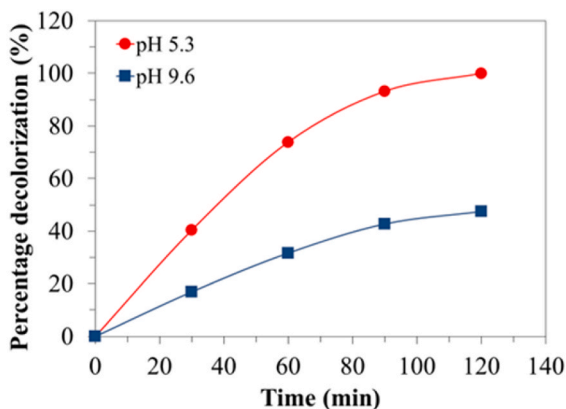


Fig. 5. Photodegradation of methyl orange solution at pH values of 5.3 and 9.6.

solution was fully degraded at 120 min. The low photocatalytic reaction in the basic condition may be due to the presence of electrostatic repulsion force between dyes and photocatalyst and at the same time was inhibited by the photocatalytic activity [13].

In addition to the irradiation time, the environment and system of the dye solution can significantly influence the degradation process over photocatalysts. In the initial screening studies, the 5% Sn-Fe₂O₃ catalyst demonstrated remarkable performance in the degradation of methyl orange. Building upon this observation, further investigations were conducted to examine the effects of pH value and dye concentration on the decolorization rate, with a focus on the degradation of methyl orange using a dye concentration of 10 ppm.

The influence of different pH values on the percentage of methyl orange decolorization is presented in Fig. 5. The results reveal that the acidic condition (pH 5.3) enhanced the degradation of the dye more effectively compared to the basic condition (pH 9.6) in the presence of the Fe₂O₃-doped Sn catalysts. Under acidic conditions, the dye solution was fully degraded within 120 min. This finding suggests that the acidic environment promotes the photocatalytic degradation process, leading to a faster decolorization of methyl orange. On the other hand, the lower photocatalytic reaction observed in the basic condition can be attributed to the presence of electrostatic repulsion forces between the dyes and the photocatalyst. Additionally, the photocatalytic activity itself may be inhibited under basic conditions [13]. These factors contribute to the reduced efficiency of the degradation reaction in the basic pH environment. The findings highlight the importance of considering the pH of the system when utilizing Fe₂O₃-doped Sn catalysts for the degradation of methyl orange.

Overall, the results emphasize the significance of both the catalyst composition and the reaction conditions in achieving efficient photocatalytic degradation of organic dyes. The 5% Sn-Fe₂O₃ catalyst demonstrated superior performance in the degradation of methyl orange, particularly under acidic conditions, where complete degradation was achieved within 120 min. Understanding the interplay between the catalyst, dye concentration, and pH value is crucial for optimizing the photocatalytic degradation process and designing effective treatment strategies for organic pollutant removal.

3.3. Effect of methyl orange concentration

By fixing the pH value at 5.3 in the presence of 5% Sn-Fe₂O₃ catalyst, the effects of 5, 10, and 20 ppm dye concentrations were studied to evaluate the photocatalytic ability of the catalyst in methyl orange degradation. Results from this study were plotted and shown in Fig. 6. Generally, methyl orange solution at high concentration requires more time to fully degrade. Thus, methyl orange at a concentration of 10 ppm yielded a rapid degradation rate compared with other concentrations of 5 or 20 ppm due to different absorptions of light.

In general, the degradation rate of dyes were fast in solutions with high concentration. This phenomenon maybe due to the high number of dye molecules, which can react with the free radicals that was produced by the photocatalysts [14,15]. Interestingly, photodegradation performance at dye concentration of 10 ppm were higher than the dyes at higher concentration of 20 ppm. This result was because the high concentration of methyl orange can reduce light penetration and absorption by the catalysts. High concentration of methyl orange reduced the generation of hole-electron and slowed down the photodegradation activities [16,17]. The low concentration of dye solution of 5 ppm showed a slightly decreased reaction. This effect may due to the presence of small amounts of methyl orange molecule that may have reduced the collisions between dye molecules and photocatalyst particles or the free radicals that have been formed.

For comparison, a variety of previously reported dopants that were incorporated into Fe₂O₃ photocatalyst are summarized in Table 2. It was found that the developed sample in this work also demonstrates excellent performance and comparable photocatalytic activity for dye degradation. Additionally, it is worth to note that the significant difference in experiment data among these studies might be influenced by different parameters that were used in the experiments. This includes type of dopant, amount of photocatalyst, volume of dye and light source.

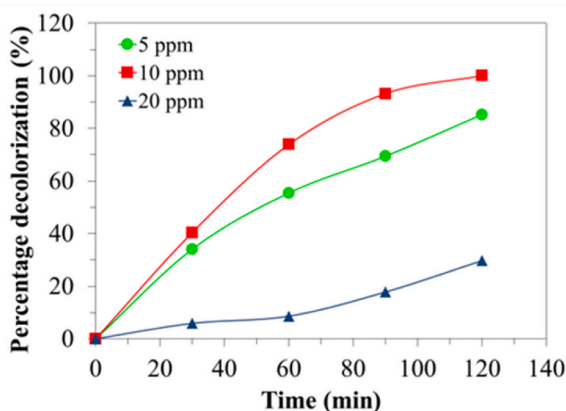


Fig. 6. Photodegradation performance of dye solutions at different concentrations of 5, 10, and 20 ppm.

Table 2A comparison table on the photocatalytic dye degradation using doped-Fe₂O₃ photocatalyst.

Dopant	Optimum dopant percentage (%)	Dye	Dye concentration	Irradiation time (min)	Photodegradation efficiency (%)	Ref
Co	4	Methylene blue	–	120	92	[18]
Co	5	Pararosaniline	5×10^{-5} M	60	89.8	[19]
Zn	4	Rose bengal	5 ppm	90	87	[20]
In ₂ O ₃	10	Rhodamine B	100 mg/L	12	94	[21]
Ca	5	Rhodamine B	10 mg/L	120	99	[22]
Zn	6	Methyl orange	10 mg/L	140	87.4	[23]
Mg	3	Methylene blue	5 mg/mL	180	90	[24]
I	1	Methylene blue	10^{-5} M	45	97.72	[25]
Sn	6	Methylene blue	–	150	92	[26]
Sn	5	Methyl orange	10 ppm	120	100	Current study

3.4. Stability and reusability of Sn-doped Fe₂O₃ photocatalysts

To evaluate the stability, the Sn-doped Fe₂O₃ photocatalysts were subjected to multiple cycles of methyl orange degradation under simulated solar light irradiation. The results showed that the catalysts maintained their high photocatalytic activity even after several cycles, indicating good stability. This stability is essential for long-term applications, as it ensures the consistent and reliable performance of the catalysts over extended periods.

Furthermore, the reusability of the catalysts was assessed by recovering the Sn-doped Fe₂O₃ particles after each degradation cycle and reusing them in subsequent cycles. The catalysts were carefully separated from the reaction solution, washed, and dried before being used again. The results demonstrated that the Sn-doped Fe₂O₃ photocatalysts retained their photocatalytic activity even after multiple reuses, indicating their potential for cost-effective and environmentally friendly applications. The stability and reusability of photocatalysts are crucial factors for their practical implementation. A catalyst that can maintain its activity over multiple cycles and can be reused without significant loss of performance is desirable from an economic and environmental perspective. The findings of this study highlight the stability and reusability of Sn-doped Fe₂O₃ photocatalysts, supporting their potential for real-world applications in wastewater treatment and other environmental remediation processes.

By investigating the stability and reusability of the catalysts, this research contributes to a comprehensive understanding of the practical feasibility and sustainability of Sn-doped Fe₂O₃ photocatalysts, further enhancing their value as efficient and reusable materials for pollutant degradation.

4. Conclusions

In this study, α -Fe₂O₃, γ -Fe₂O₃, and Fe₂O₃ doped with varying percentages of Sn dopant were successfully synthesized using the sol-gel method. The introduction of Sn dopant loading, up to 5%, led to a decrease in the bandgap energy of Fe₂O₃ by approximately 0.1 eV. This reduction in bandgap energy indicates improved light absorption ability and enhanced formation of electron-hole pairs, which significantly enhanced the photodegradation performance of Sn-doped Fe₂O₃ photocatalysts.

The presence of a small amount (5%) of Sn dopant on Fe₂O₃ showed enhanced photodegradation of methyl orange, resulting in the formation of less toxic secondary products. The addition of Sn species played a crucial role in decreasing the bandgap value of the Sn-doped Fe₂O₃ photocatalysts, thereby improving their light absorption capability. This enhancement in light absorption, coupled with efficient formation of electron-hole pairs, contributed to the improved photodegradation performance of the catalysts.

The optimum conditions for photodegradation using 5% Sn-doped Fe₂O₃ were found to be a methyl orange concentration of 10 ppm and an acidic environment. Under these conditions, complete degradation of methyl orange was achieved within 120 min. The acidic condition was found to enhance the photodegradation process more effectively compared to the alkaline condition. This suggests that the pH of the system plays a critical role in influencing the photocatalytic degradation efficiency. Furthermore, the concentration of methyl orange also exerted a significant effect on the light absorption of the photocatalyst, which directly affected the maximum color removal percentage. At higher concentrations of methyl orange (20 ppm), the photodegradation rate dramatically decreased due to insufficient active sites for reaction. This observation suggests that the number of substrate ions accommodated in the inter-layer space increased with increasing dye concentration, leading to a reduction in the degradation of methyl orange.

In summary, this study successfully synthesized Sn-doped Fe₂O₃ photocatalysts with improved light absorption and enhanced photodegradation performance. The presence of Sn dopant reduced the bandgap energy, allowing for efficient degradation of methyl orange into less toxic products. The optimal conditions for photodegradation were identified as an acidic environment with a methyl orange concentration of 10 ppm. These findings contribute to the understanding of the factors influencing the photocatalytic degradation process and provide valuable insights for the design and development of efficient photocatalysts for organic pollutant removal.

Author contribution statement

Nurul Affiqah Arzaee, Nadia Betti: Conceived and designed the experiments; Contributed reagents, materials, analysis tools or data; Wrote the paper.

Ahmed Al-Amiry: Performed the experiments; Contributed reagents, materials, analysis tools or data; Wrote the paper.

Wan Nor Roslam Wan Isahak: Analyzed and interpreted the data; Contributed reagents, materials, analysis tools or data; Wrote the paper.

Data availability statement

Data will be made available on request.

Declaration of competing interest

The authors declare that they have no known competing financial interests or personal relationships that could have appeared to influence the work reported in this paper.

Acknowledgments

The authors wish to thank Universiti Kebangsaan Malaysia (UKM) for funding this project under research grant GUP-2020-012 and the Centre of Research and Innovation Management (CRIM) UKM for the use of the instruments.

References

- [1] S. Lam, J. Sin, A.Z. Abdullah, A.R. Mohamed, Degradation of wastewaters containing organic dyes photocatalyzed by zinc oxide: a review, *Desalination Water Treat.* 41 (2012) 131–169, <https://doi.org/10.1080/19443994.2012.664698>.
- [2] F. Su, P. Li, J. Huang, M. Gu, Z. Liu, Y. Xu, Photocatalytic degradation of organic dye and tetracycline by ternary Ag₂O/AgBr–CeO₂ photocatalyst under visible-light irradiation, *Sci. Rep.* 11 (2021), <https://doi.org/10.1038/s41598-020-76997-0>. Article number 85.
- [3] F. Huang, A. Yan, H. Zhao, *Semiconductor Photocatalysis - Materials, Mechanisms and Applications*, 2016 (InTech publisher).
- [4] S. Zhang, F. Ren, W. Wu, J. Zhou, X. Xiao, L. Sun, Y. Liu, et al., Controllable synthesis of recyclable core–shell γ -Fe₂O₃@SnO₂ hollow nanoparticles with enhanced photocatalytic and gas sensing properties, *Phys. Chem. Chem. Phys.* 15 (2013) 8228–8236, <https://doi.org/10.1039/C3CP50925G>.
- [5] G. Mamba, A. Mishra, Advances in magnetically separable photocatalysts: smart, recyclable materials for water pollution mitigation, *Catalysts* 6 (12) (2016) 79, <https://doi.org/10.3390/catal6060079>.
- [6] M. Mishra, D.-M. Chun, α -Fe₂O₃ as a photocatalytic material: a review, *Appl. Catal. Gen.* 498 (2015) 126–141, <https://doi.org/10.1016/j.apcata.2015.03.023>.
- [7] Z. Cao, M. Qin, Y. Gu, B. Jia, P. Chen, X. Qu, Synthesis and characterization of Sn-doped hematite as visible light photocatalyst, *Mater. Res. Bull.* 77 (2016) 41–47, <https://doi.org/10.1016/j.materresbull.2016.01.004>.
- [8] Z.A.C. Ramli, N. Asim, W.N.R.W. Isahak, Z. Emdadi, N.A. Ludin, M.A. Yarmo, K. Sopian, Photocatalytic degradation of methylene blue under UV light irradiation of prepared carbonaceous TiO₂, *Sci. World J.* (2016), <https://doi.org/10.1155/2014/415136>. Article ID 415136.
- [9] J. Safaei, H. Ullah, N.A. Mohamed, M.F.M. Noh, M.F. Soh, A.A. Tahir, N.A. Ludin, M.A. Ibrahim, W.N.R.W. Isahak, M.A.M. Teridi, Enhanced photoelectrochemical performance of Z-scheme g-C₃N₄/BiVO₄ photocatalyst, *Appl. Catal. B Environ.* 234 (2018) 296–310, <https://doi.org/10.1016/j.apcatb.2018.04.056>.
- [10] S. Em, M. Yedigenov, L. Khamkhash, A. Molkenova, T.S. Atabaev, Sn-doped hematite nanoparticles for potential photocatalytic dye degradation, *IOP Conf. Ser. Mater. Sci. Eng.* 739 (2020), 012042, <https://doi.org/10.1088/1757-899X/739/1/012042>.
- [11] Keerthanam S. P.; Yuvakkumar, R.; Ravi, G.; Kumar, P.; Elshikh, M. S.; Alkhamis, H. H.; Alrefaei, A. F.; Velauthapillai, D. A strategy to enhance the photocatalytic efficiency of α -Fe₂O₃, *Chemosphere*, 270, pp. 129498. DOI: <https://doi.org/10.1016/j.chemosphere.2020.129498>.
- [12] M. Soltys-Mroz, K. Syrek, J. Pierzchala, E. Wiercigroch, K. Malek, G.D. Sulka, Band gap engineering of nanotubular Fe₂O₃-TiO₂ photoanodes by wet impregnation, *Appl. Surf. Sci.* 517 (2020), 146195, <https://doi.org/10.1016/j.apsusc.2020.146195>.
- [13] P.V. Korake, A.N. Kadam, K.M. Garadkar, Photocatalytic activity of Eu³⁺-doped ZnO nanorods synthesized via microwave assisted technique, *J. Rare Earths* 32 (2014) 306–313, [https://doi.org/10.1016/S1002-0721\(14\)60072-7](https://doi.org/10.1016/S1002-0721(14)60072-7).
- [14] T. Lupascu, M. Ciobanu, O. Bogdevici, V. Botan, Products derived from catalytic oxidation of methylene blue, *Chemistry J. Maldova* 6 (2011) 77–80, [https://doi.org/10.19261/cjm.2011.06\(1\).07](https://doi.org/10.19261/cjm.2011.06(1).07).
- [15] J. Safaei, N.A. Mohamed, M.F.M. Noh, M.F. Soh, N.A. Ludin, M.A. Ibrahim, W.N.R.W. Isahak, M.A.M. Teridi, Graphitic carbon nitride (g-C₃N₄) electrodes for energy conversion and storage: a review on photoelectrochemical water splitting, solar cells and supercapacitors, *J. Mater. Chem.* 6 (2018) 22346–22380.
- [16] J. Safaei, N.A. Mohamed, M.F.M. Noh, M.F. Soh, A.M. Elbreki, N.A. Ludin, M.A. Ibrahim, A.H.A. Al-Waeli, W.N.R.W. Isahak, M.A.M. Teridi, Simultaneous enhancement in light absorption and charge transportation of bismuth vanadate (BiVO₄) photoanode via microwave annealing, *Mater. Lett.* 233 (2021) 67–70.
- [17] K.B. Ghoreishi, N. Asim, Z.A.C. Ramli, Z. Emdadi, M.A. Yarmo, Highly efficient photocatalytic degradation of methylene blue using carbonaceous WO₃/TiO₂ composites, *J. Porous Mater.* 23 (2021) 629–637.
- [18] S.P. Keerthana, R. Yuvakkumar, G. Ravi, P. Kumar, M. Elshikh, H. Alkhamis, A. Alrefaei, D. Velauthapillai, A strategy to enhance the photocatalytic efficiency of α -Fe₂O₃, *Chemosphere* 270 (2021), 129498.
- [19] R. Suresh, K. Giribabu, R. Manigandan, R.V. Mangalaraja, Jorge Yanez Solorza, A. Stephen, V. Narayanan, Synthesis of Co²⁺-doped Fe₂O₃ photocatalyst for degradation of pararosaniline dye, *Solid State Sci.* 68 (2017) 39–46.
- [20] Surjeet Chahal Suman, Ashok Kumar, Parmod Kumar, Zn doped α -Fe₂O₃: an efficient material for UV driven photocatalysis and electrical conductivity, *Crystals* 10 (4) (2020) 273, <https://doi.org/10.3390/cryst10040273>.
- [21] Nan Guo, Haiyan Liu, Yong Fu, Jianshe Hu, Preparation of Fe₂O₃ nanoparticles doped with In₂O₃ and photocatalytic degradation property for rhodamine B, *Optik* 201 (2020), 163537.
- [22] Sheng Guo, Haojie Wang, Wei Yang, Fida Hussain, Liming You, Kun Zhou, Scalable synthesis of Ca-doped α -Fe₂O₃ with abundant oxygen vacancies for enhanced degradation of organic pollutants through peroxymonosulfate activation, *Appl. Catal. B Environ.* 262 (2020), 118250.
- [23] A. Lassoud, Synthesis and characterization of Zn-doped α -Fe₂O₃ nanoparticles with enhanced photocatalytic activities, *J. Mol. Struct.* 1239 (2021), 130489.

- [24] Ayed, Rihab Ben, Mejda Ajili, Yolanda Piñero, Badriyah Alhalaili, José Rivas, Ruxandra Vidu, Salah Kouass, Najoua Kamoun Turki, Effect of Mg doping on the physical properties of Fe₂O₃ thin films for photocatalytic devices, *Nanomaterials* 12 (7) (2022) 1179, <https://doi.org/10.3390/nano12071179>.
- [25] Selim Demirci, Yurddaskal Metin, Tuncay Dikici, Cevat Sarıoğlu, Fabrication and characterization of novel iodine doped hollow and mesoporous hematite (Fe₂O₃) particles derived from sol-gel method and their photocatalytic performances, *J. Hazard Mater.* 345 (2018).
- [26] Houda Mansour, Radhouane Bargougui, Cécile Autret-Lambert, Abdellatif Gadri, Salah Ammar, Co-precipitation synthesis and characterization of tin-doped α-Fe₂O₃ nanoparticles with enhanced photocatalytic activities, *J. Phys. Chem. Solid.* 114 (2018) 1–7.